Available online at www.sciencedirect.com
SCIENCE DIRECT®
International Journal of Pharmaceutics 288 (2005) 361–368
international journal of pharmaceutics
www.elsevier.com/locate/ijpharm

In vitro and in vivo evaluation of actively targetable nanoparticles for paclitaxel delivery

Zhenghong Xu[a,c], Wangwen Gu[a], Jun Huang[a,b], Hong Sui[a], Zhaohui Zhou[d], Yongxin Yang[a,b], Zhou Yan[a,b], Yaping Li[a,*]

[a] *Shanghai Institute of Materia Medica, Shanghai Institute for Biological Sciences, Chinese Academy of Sciences, 555 Zuchongzhi Road, Shanghai 201203, China*
[b] *School of Pharmacy, Fudan University, Shanghai 200032, China*
[c] *Graduate School of the Chinese Academy of Sciences, China*
[d] *Onlly Limited Corporation, Shanghai Jiaotong University, Shanghai 200030, China*

Received 18 August 2004; received in revised form 20 October 2004; accepted 24 October 2004

Abstract

The aim of the present work was to assess the merits of an actively targetable nanoparticles (ATN), PEG-coated biodegradable polycyanoacrylate nanoparticles (PEG-nanoparticles) conjugated to transferrin, for paclitaxel delivery. PEG-nanoparticles loading paclitaxel were prepared by solvent evaporation technique in advance. ATN were prepared by coupling of transferrin to PEG-nanoparticles. The results showed that the average encapsulation efficiency of ATN was $93.4 \pm 3.6\%$ with particle size (101.4 ± 7.2 nm) and zeta-potential (-13.6 ± 1.1 mV). The paclitaxel loaded ATN exhibited a low burst effect with about only 16.2% drug release within the first phase. Subsequently, paclitaxel release profiles displayed a sustained release phase. The amount of cumulated paclitaxel release over 30 days was 81.6%. ATN exhibited a markedly delayed blood clearance in mice, and the paclitaxel level from ATN remained much higher at 24 h compared with that of free drug from paclitaxel injection. The distribution profiles of ATN in S-180 solid tumor-bearing mice after intravenous administration showed the tumor accumulation of paclitaxel increase with time, and the paclitaxel concentration in tumor was about 4.8 and 2.1 times higher than those from paclitaxel injection and PEG-nanoparticles at 6 h after intravenous injection. For mice treated with 20 mg/kg × 5 of ATN, the decrease in body weight was limited within 4% of the initial weight at 5 days after the final administration, and tumor regression was significantly observed with complete tumor regression for five out of nine mice. The tumor burden with ATN-treated mice was much smaller compared with free paclitaxel or NTN-treated mice. In addition, the life span of tumor-bearing mice was significantly increased when they were treated with ATN, in particular, three mice survived over 60 days. Thus, PEG-coated biodegradable polycyanoacrylate nanoparticles conjugated to transferrin could be an effective carrier for paclitaxel delivery.
© 2004 Elsevier B.V. All rights reserved.

Keywords: Paclitaxel; Nanoparticles; Drug delivery; Polyethylene glycol; Transferrin

* Corresponding author. Tel.: +86 21 5080 6820; fax: +86 21 5080 6820.
E-mail address: ypli@mail.shcnc.ac.cn (Y. Li).

0378-5173/$ – see front matter © 2004 Elsevier B.V. All rights reserved.
doi:10.1016/j.ijpharm.2004.10.009

1. Introduction

Paclitaxel has demonstrated significant activity in clinical trials against a wide variety of tumors, especially, ovarian and breast cancer in the past 10–20 years. However, due to its high hydrophobicity, an adjuvant such as Cremophor EL has to be used to prepare injection as its clinical dosage form. Unfortunately, Cremophor EL causes serious side-effects and leads to hypersensitivity reactions in many patients (Panchagnula, 1998; Dhanikula and Panchagnula, 1999; Singla et al., 2002). In order to increase therapeutic efficiency and reduce side-effects, much effort has been devoted to the development of tumor-targetable DDS of paclitaxel such as liposomes (Sampedro et al., 1993; Sharma and Straubinger, 1994; Crosasso et al., 2000), nanoparticles (Suh et al., 1998; Fonseca et al., 2002; Mu and Feng, 2002, 2003; Kim et al., 2003; Mitra and Lin, 2003; Potineni et al., 2003), parenteral emulsion (Lundberg, 1997; Kan et al., 1999), water-soluble prodrugs and conjugates (Rodrigues et al., 1995; Dosio et al., 1997; Pendri et al., 1998; Safavy et al., 2003). So far, the different approaches investigated have shown a lot of promise to replace the Cremophor EL-based vehicle for paclitaxel delivery, but except liposomes, the final product for human use is still far away.

In general, solid tumors show hypervascular permeability and impaired lymphatic drainage. Due to such effects, macromolecules or nanoparticles (<200 nm) can significantly accumulate in tumor, however, this behavior belongs to passive mechanism and lacks goaheadism to recognize and bind to tumor cell or tissue. It has been reported that the membrane transferrin receptor-mediated endocytosis of the complex of transferrin bound iron and transferrin receptor is the major route of cellular iron uptake, and the efficient cellular uptake pathway has been exploited for the site-specific delivery of anti-tumor drugs, protein and therapeutic gene into proliferating cells including erythroblasts and cancer cells that overexpress transferrin receptor (Wagner et al., 1994; Li and Qian, 2002). The conjugation of transferrin with drugs is usually performed either directly by chemical conjugation or genetically by infusion of peptides/proteins into the structure of transferrin. Although direct coupling methods are easy to carry out, they show some disadvantages, such as polymeric products are likely to be formed during the preparation, and the resulting conjugates are chemically poorly defined with respect to the chemical link between drugs and carrier proteins (Kratz and Beyer, 1998; Singh, 1999). In addition, it has shown that transferrin-coupled liposomes significantly enhanced uptake of free doxorubicin or α-IFN via the receptor-mediated mechanism (Liao et al., 1998; Eavarone et al., 2000). So, the design of PEG-coated biodegradable polycyanoacrylate nanoparticles conjugated to transferrin (transferrin-PEG nanoparticles), an actively targetable nanoparticles (ATN) as paclitaxel carriers could be one of the ideal solutions to deliver paclitaxel to tumor because ATN has double effect from passive and active mechanism.

Previously, we prepared nanoparticles bearing polyethylene glycol-coupled transferrin for delivery of pDNA, and the cells association assay showed that the degree of target cell binding of this nanoparticles was much greater than that of common PEG-nanoparticles without bearing transferrin in vitro (Li et al., 2003). In this study, we selected paclitaxel as model drug and compared ATN's pharmacokinetics behavior, distribution, toxicity and anti-tumor efficacy in animal models with non-actively targeted PEG-nanoparticles (NTN) and current clinical formulation (paclitaxel injection). The result showed that this new formulation achieved a lot of advantages, especially, more effectively tumor regression through remarkably enhanced tumor accumulation of paclitaxel.

2. Materials and methods

2.1. Materials

Paclitaxel (purity, >99%) and paclitaxel injection (No. 030911, 30 mg/5 ml) were purchased from Shanghai Hualian Pharmaceutical Co. Ltd. t-Boc-HNPEG 3400 was purchased from Shearwater Polymers Inc. (Huntsville, AL). Cyanoacetic acid (purity, 99%) and polyvinylalcohol (MW = 16,000) was obtained from Fluka (Buches, Switzerland). *n*-Hexadecanol, trifluoroacetic acid and human transferrin were purchased from Sigma (St. Louis, MO,USA). Mouse-anti-human transferrin antibody (MAB 033-19/1) and Goat-anti-mouse IgG antibody (Alexa Fluor® 488, A-11001) was purchased from Molecular Probes (Eugene, OR, USA). Poly(aminopoly(ethylene glycol)cyanoacrylate-co-hexadecyl cyanoacrylate)

(poly(H_2NPEGCA-co-HDCA)) was synthesized according to the methods from Stella et al. (Stella et al., 2000). Dichloromethane and acetonitrile of HPLC grade was used in this study. All other reagents and solvents were of an analytical grade.

2.2. Animals

Female Kunming strain mice (20 ± 2 g) were supplied by the Shanghai Experimental Animal Center, Chinese Academy of Sciences (Shanghai, China). The animal were acclimatized at a temperature of $25 \pm 2\,^{\circ}C$ and a relative humidity of $70 \pm 5\%$ under natural light/dark conditions for 1 week before dosing.

2.3. Preparation of ATN loading paclitaxel

Poly(H_2NPEGCA-co-HDCA) nanoparticles (non-actively targeted PEG-nanoparticles, NTN) loading paclitaxel were prepared by solvent evaporation technique in advance. Briefly, 0.6 ml of paclitaxel (30 mg) in dichloromethane containing poly(H_2NPEGCA-co-HDCA) (100 mg) was emulsified in 2 ml of polyvinylalcohol aqueous solution (0.5%, w/v) by sonification for 10 s (Sonifier 250, Branson, output = 10 units) to form primary emulsion (O/W). Then, the emulsion (O/W) was diluted in 20 ml polyvinylalcohol solution (0.1%, w/v) under moderate magnetic stirring. The magnetic stirring was maintained for over 1 h to allow solidification of the nanoparticles at 25 °C. The organic solution was eliminated by evaporation under reduced pressure (Rotavapor R-114, Bűchi, Switzerland) at 37 °C. Finally, the nanoparticles were collected by centrifugation at $35{,}000 \times g$ for 20 min (Beckman Model J2-21) and washed twice with water before lyophilization.

ATN were prepared by coupling of transferrin to PEG-nanoparticles using our previous method (Li et al., 2003). Briefly, the solution of transferrin (100 mg) in 1 ml of 30 mM sodium acetate buffer (pH 5) was mixed with 50 μl of 30 mM sodium acetate buffer (pH 5.0) containing 1.5 mg of sodium periodate. The mixture was left to stand for 90 min in an ice bath in the dark. Then, gel filtration was carried out in Sephadex G-25 PD 10 column (Pharmacia, 150 mM NaCl, 10 mM HEPES, pH 7.3), whereupon 1 ml of a solution containing 80 mg of oxidized transferrin was obtained. The content of oxidized aldehyde-containing form of transferrin was determined by absorption measurement at 280 nm. Some of the modified transferrin solution (0.5 μmol) was added quickly to a solution containing 10 mg of NTN loading paclitaxel in 0.5 ml of HBS. After 12 h at ambient temperature, ATN were purified to remove excess free transferrin by diluting ATN with an equal volume of HBS (150 mM NaCl, 20 mM HEPES, pH 7.4) and centrifuging at $35{,}000 \times g$ for 20 min (Beckman Model J2-21). The quantitative measurement of the transferrin bound to PEG-nanoparticles was done according to our previous methods (Li et al., 2003).

2.4. Physicochemical characteristics of ATN loading paclitaxel

The morphological examination of ATN was performed using a transmission electron microscope (TEM, CM12 Philips, Netherlands) following negative staining with sodium phosphotungstate solution (0.2%, w/v). Size, size distribution and ζ potential of nanoparticles were measured by laser light scattering following their resuspension in water using a Nicomp 380/ZLS zeta potential analyzer (Particle Sizing Systems, USA). The entrapment efficiency was obtained by measuring the amount of paclitaxel that was encapsulated in ATN. The paclitaxel encapsulated in nanoparticles was determined by adding 10 mg of ATN to 2 ml of dichloromethane and shaking, then 4 ml of a mixture of CH_3CN:H_2O (1:1,v/v) was added. A nitrogen stream was introduced to evaporate dichloromethane. The amount of paclitaxel was determined by HPLC method following experimental conditions: Diamond® C_{18} column (150 mm × 4.6 mm i.d., pore size 5 μm); the mobile phase, CH_3CN:H_2O (1:1,v/v); flow rate, 1.0 ml/min; and measured wavelength: 227 nm with UV detector.

2.5. In vitro release experiment

Release experiment was carried out in 30 mM phosphate buffer (pH 7.4). Two hundred milligrams of nanoparticles was suspended in 15 ml of phosphate buffer at 37 °C under horizontal shaking (100 rpm). For comparison, a release evaluation of NTN was also performed. At predetermined time intervals, the suspension of nanoparticles was centrifuged and the supernatant collected for further paclitaxel analysis. The

nanoparticles were resuspended in the same volume of fresh medium and incubated again under the same conditions. The amount of paclitaxel released in each time interval was determined by HPLC assay as previously described for measurement of encapsulation efficiency.

2.6. Pharmacokinetics and biodistribution in mice

Pharmacokinetics and biodistribution studies were performed using Kunming strain mice with S-180 tumor nodules of 9–10 mm in diameter. For comparison, the pharmacokinetic and biodistribution evaluation of NTN and the paclitaxel injection were also performed. For administration, nanoparticles were suspended in a certain volume of PBS (pH 7.4) in order to obtain the required concentration. The different formulations were injected through the tail vein at the paclitaxel dose of 20 mg/kg mouse, and each group consisted of 8–10 animals. For pharmacokinetic experiment, blood samples were taken at 0.25, 0.5, 1.0, 2.0, 4.0, 6.0, 8.0, 12 and 24 h from the retro orbital plexus. Serum samples were harvested by centrifugation, and drug was extracted with *tert*-butyl methyl ether on a vortex mixer. After centrifugation, the organic layer was transferred to another clean test tube and evaporated, and the residue was analyzed by HPLC following experimental conditions: Diamond® C_{18} column (150 mm × 4.6 mm i.d., pore size 5 μm); the mobile phase, CH_3CN:H_2O (1:1,v/v); flow rate, 1.0 ml/min; and measured wavelength: 227 nm. Pharmacokinetic parameters were obtained using the Practical Pharmacokinetic Program-Version 87. For biodistribution experiment, the animals were scarificed after defined time periods, and then tissue was harvested and stored at −50 °C until analyzed for paclitaxel.

2.7. In vivo anti-tumor activity

In vivo anticancer activity was evaluated against S-180-bearing KM mice (female, 6 weeks old, $n = 8$–10). Mice were inoculated subcutaneously into the armpit with S-180 cells. After 7 days, paclitaxel injection and nanoparticles suspensions were given by intravenous injection each second day (five times) at a dose of 20 mg/kg/day for 10 days. Group 1 was treated with saline, groups 2–4 with paclitaxel injection, ATN and NTN. Body weight and tumor volume ([major axis] × [minor axis]^2 × 1/2) were measured at defined time periods. Statistical evaluation of tumor volume was analyzed by using Student's *t*-test.

3. Results and discussion

3.1. Characteristics of ATN loading paclitaxel

The characteristics of ATN loading paclitaxel were summarized in Table 1. The paclitaxel was incorporated in ATN and NTN with a little different encapsulation efficiency by emulsion technique. ATN showed slightly low encapsulation efficiency than that of NTN. This result could be from that some paclitaxel was unadsorbed during transferrin was conjugated with NTN. In general, some of the drug could be adsorbed onto the surface of the nanoparticles by various forces such as Vander Wals forces etc. When transferrin was conjugated with NTN, some of the transferrin could be unadsorbed and left surface of the nanoparticles into solution. As a result, ATN showed slightly low encapsulation efficiency than that of NTN. However, the encapsulation efficiency of ATN and NTN did not show significant difference ($P > 0.05$). ATN observed by TEM showed spherical in shape (Fig. 1). The particle size is one of the most important properties of nanoparticles drug delivery system because particle size shows a great effect on drug release characteristics and drug distribution in different organs of the body, particularly, tumor tissues. It has been reported that solid tumors show hypervascular permeability and impaired lymphatic drainage. As a result, liposomes or nanoparticles (<200 nm) can significantly accumulate in tumor by "filtration" mechanism (Iodoshima et al., 1997). In addition, injectable nanoparticles also can not too large to pass through a syringe needle. The particle size of ATN is no more than 120 nm. The ATN loading paclitaxel exhibited a negative surface charge (−13.6 ± 1.1 mV). However, the particle size and surface charge of ATN

Table 1
The characteristics of ATN loading paclitaxel

	Entrapment efficiency (%)	Particle size (nm)	Zeta-potential (mV)
ATN	93.4 ± 3.6*	101.4 ± 7.2*	−13.6 ± 1.1
NTN	98.2 ± 3.3	91.6 ± 6.1	−14.1 ± 2.3

Mean ± S.D., each batch was measured in triplicate.
* $P > 0.05$, statistical significance compared with NTN group.

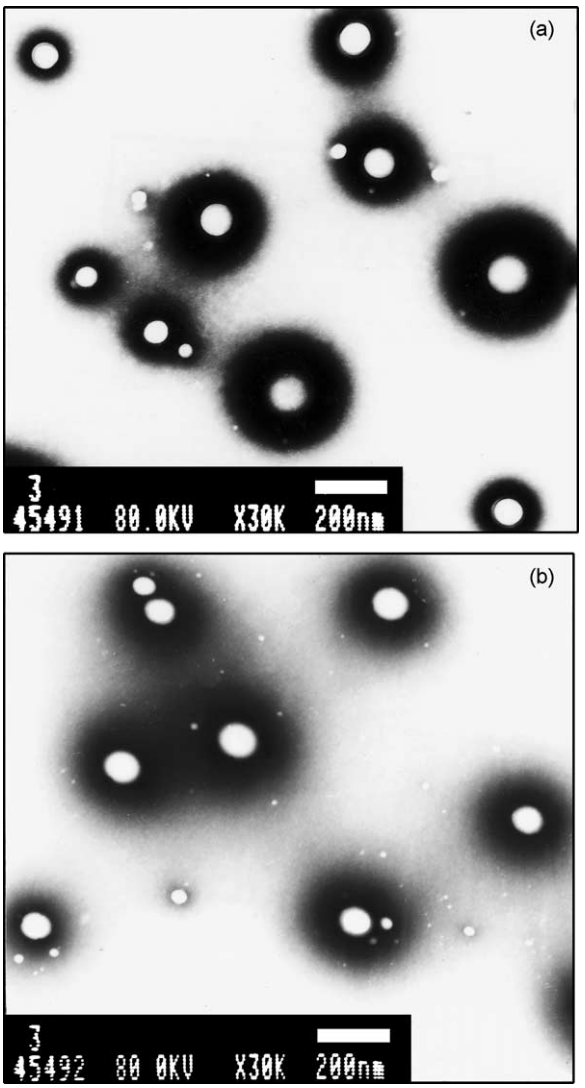

Fig. 1. Transmission electron micrographs of ATN (a) and NTN (b).

and NTN did not show significant difference ($P > 0.05$). To evaluate the extent of transferrin conjugation in ATN loading paclitaxel, the coupling efficiency of transferrin was estimated by quantitative analysis that was performed after rinse of the conjugate. PEG chains were calculated by the assumption that the molecular weight of transferrin is 80,000. It was found that 5–8% of the total PEG chains were linked to transferrin molecules.

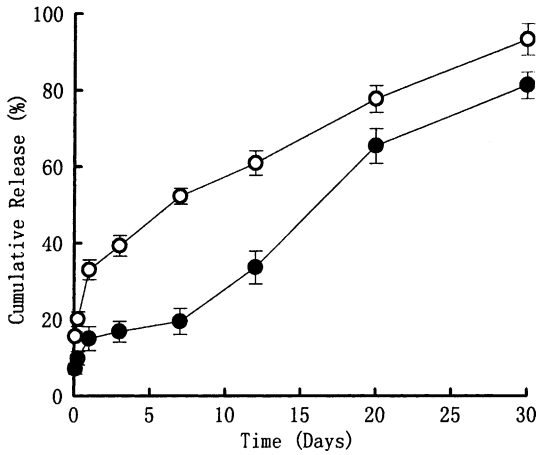

Fig. 2. Release of paclitaxel from ATN (●) and NTN (○). Data were given as mean ± S.D. for $n = 3$.

3.2. In vitro release experiments

The in vitro release profiles of paclitaxel were obtained by representing the percentage of paclitaxel release with respect to the amount of paclitaxel loaded in nanoparticles (Fig. 2). The paclitaxel loaded ATN exhibited a low burst effect with about only 16.2% drug release within the first day. After 1 day, paclitaxel release profiles displayed a sustained release phase. The amount of cumulated paclitaxel release over 30 days was 81.6%. This sustained release could mainly result from the erosion and degradation of the polymer because paclitaxel has very poor dissolution in water. Compared with ATN, the amount of cumulated paclitaxel release from NTN over 30 days was 93.2%. The in vitro release profiles of paclitaxel loaded in ATN and NTN showed a slight difference, mainly, NTN exhibited a little high burst effect with about 33.6% drug release within 1 day. As described above, during preparation of ATN, transferrin must be conjugated with NTN, some of drug could be unadsorbed and left surface of the nanoparticles into solution. In general, these paclitaxel also should belong to the part of burst release.

3.3. Pharmacokinetics and biodistribution in mice

The blood clearance curves for paclitaxel loaded in nanoparticles after intravenous injection were shown in Fig. 3. The ATN showed an initial similar blood

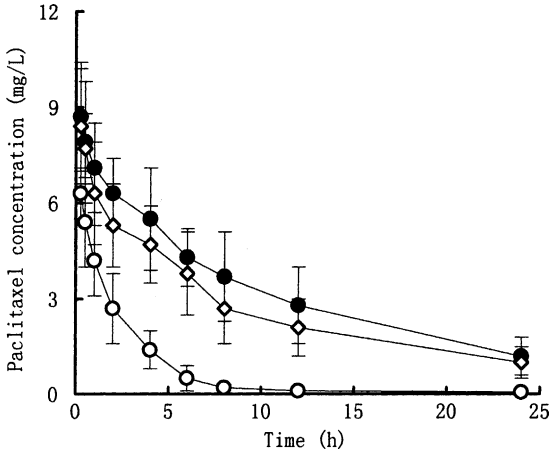

Fig. 3. Blood clearance curves of paclitaxel in ATN (◊), NTN (●) and paclitaxel injection (○). Data were given as mean ± S.D. for $n = 4$–5.

circulating levels compared with NTN at 15 min after dosing. After 15 min, free drug from paclitaxel injection was quickly removed from the circulating system. On the contrary, ATN and NTN exhibited a markedly delayed blood clearance. It could be seen that the paclitaxel level from ATN and NTN remained higher at 24 h compared with those of free drug from paclitaxel injection. This result confirmed again the idea of forming nanoparticles with a steric PEG barrier that would prevent their rapid uptake by mononuclear phagocyte system and improve their circulatory half-life as our previous experiments (Li et al., 2001a,b). The paclitaxel-time curves for ATN, NTN and injection in mice were fitted with the two-compartment model, and pharmacokinetic parameters were summarized in Table 2 . Paclitaxel loaded in NTN and ATN were eliminated rather slowly with $t_{1/2}\beta$ for NTN (7.21 h) and ATN (6.56 h). The $t_{1/2}\beta$ of NTN showed a little long than that of ATN, but $t_{1/2}\beta$ of ATN and NTN did not show significant difference ($P > 0.05$).

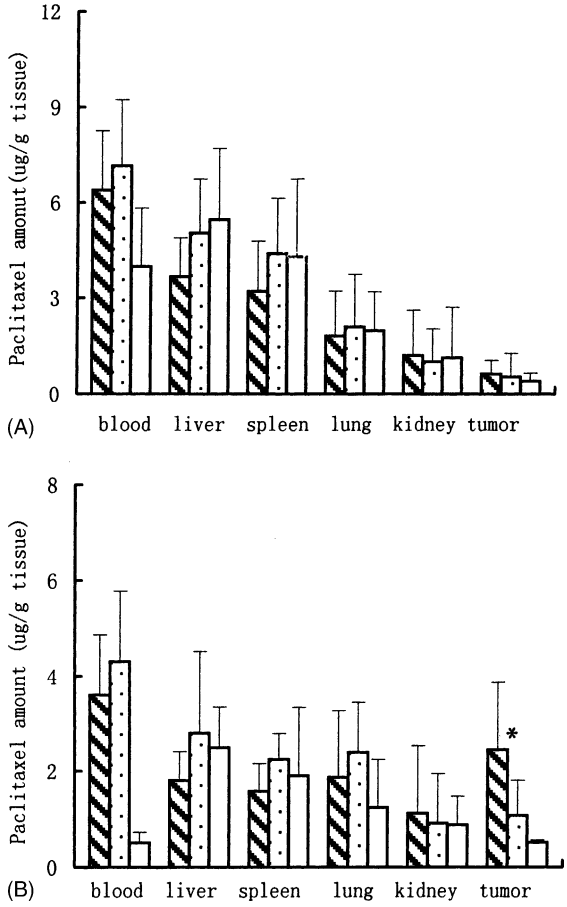

Fig. 4. Tissue distribution of paclitaxel in mice at 1 h (A) and 6 h (B), ATN (▨), NTN (⊡) and paclitaxel injection (□). Data were given as mean ± S.D. for $n = 4$–5. Statistical significance compared with NTN group: $^{*}P < 0.01$.

The distribution profiles of free drug and nanoparticles loaded with paclitaxel in S-180 solid tumor-bearing mice after intravenous administration were shown in Fig. 4. After 1 h, free paclitaxel was mainly distributed to the liver, spleen, lung and kidney. The

Table 2
Mean pharmacokinetic parameters of paclitaxel after administration of ATN, NTN and free paclitaxel

	AUC ($\mu g\,ml^{-1}\,h$)	$t_{1/2}\alpha$ (h)	$t_{1/2}\beta$ (h)	CL ($ml\,h^{-1}$)	V(c) ($ml\,kg^{-1}$)
Injection	9.62	0.14	1.29	0.83	0.21
ATN	27.55*	0.08	6.56*	0.48	1.32
NTN	31.78	0.13	7.21	0.57	1.23

Each data was from three to four mice.
* $P > 0.05$, statistical significance compared with NTN group.

tumor accumulation of free paclitaxel was very low. At 6 h after intravenous injection, free paclitaxel were gradually eliminated from all tissues. ATN and NTN were transported from the blood to normal tissues to a different extent and profile compared with free paclitaxel. The plasma levels of drug loaded in ATN and NTN were markedly higher than free paclitaxel at the same time points and their transport to the liver and kidney were found to be markedly limited. Although $t_{1/2}\beta$ of ATN and NTN showed slight difference, the paclitaxel in tumor was 4.8 and 2.1 times higher, respectively, than that of free paclitaxel from injection at 6 h after intravenous injection. ATN demonstrated higher tumor selectivity and concentration of paclitaxel in tumor than those of NTN ($P < 0.01$).

3.4. In vivo anti-tumor activity

In order to study in vivo anti-tumor activity of ATN loading paclitaxel, during preliminary experiment, S-180 cells, B16 cells and C26 cells were selected and compared for recognition and binding to ATN in vitro as our previous experiment (Li et al., 2003). However, an obvious difference among these cells did not appear (unpublished data). S-180 cells were one of the classical tumor models for a very long time, however, its characteristics including density of transferrin receptors on surface of S-180 cells still not been reported until today. For mice treated with 20 mg/kg × 5 of ATN, the decrease in body weight was limited within 4% of the initial weight, and tumor regression was significantly observed with complete tumor regression for five out of nine mice. The tumor burden with ATN-treated mice was much smaller compared with paclitaxel injection or NTN-treated mice (Fig. 5). In addition, the life span of tumor-bearing mice was significantly increased when they were treated with ATN, in particular, three out of nine mice survived over 60 days. On the other hand, for mice treated by NTN with the same dose as ATN, body weight decreased obviously, the change of body weight was about 10% of the initial weight, which showed significant difference with ATN group ($P < 0.05$), and tumor regression was also significantly observed (Fig. 5), but complete tumor regression for only two out of 10 mice. The tumor burden with NTN-treated other mice was a little small compared with free paclitaxel-treated mice. To mice treated with paclitaxel injection, a large decrease in body weight was observed. Five days after the final administration, the decrease in body weight was approximately 30% of the initial. Complete tumor regression was not observed.

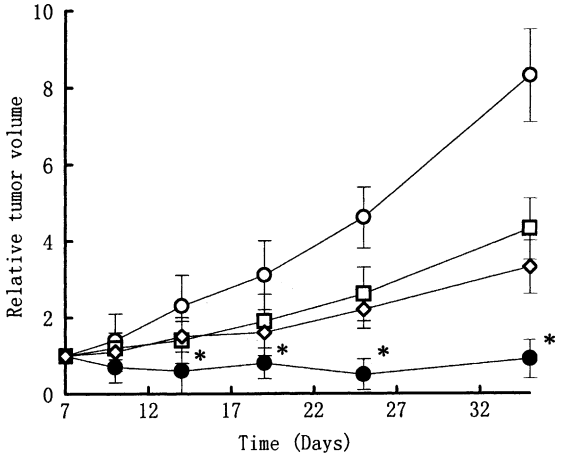

Fig. 5. Anti-tumor effects (in terms of tumor growth) of ATN (●), NTN (◊), paclitaxel injection (□) and saline (○) on S-180 solid tumors. Data were given as mean ± S.D. for $n > 4$. Statistical significance compared with NTN group: $^{*}P < 0.01$.

3.5. Conclusion

ATN loading paclitaxel could be prepared by PEG-nanoparticles conjugated to transferrin. ATN showed that the average encapsulation efficiency was over 90%. The paclitaxel loaded ATN exhibited a low burst effect within the first phase and a sustained release over 30 days. Paclitaxel loaded in ATN were eliminated rather slowly with $t_{1/2}\beta$ over 6 h. The distribution of ATN in S-180 solid tumor-bearing mice after intravenous administration showed the tumor accumulation of paclitaxel increase with time, and the paclitaxel in tumor was about 4.8 and 1.1 times higher than free paclitaxel or NTN at 6 h after intravenous injection. For mice treated with ATN, the decrease in body weight was limited, and tumor regression was significantly observed with complete tumor regression for over 50% of mice. In addition, the life span of tumor-bearing mice was significantly increased when they were treated with ATN. Thus, ATN could be a potential carrier for effective paclitaxel delivery.

Acknowledgements

The work was partly supported by the National Natural Science Foundation of China, No. 30371691, and the National Basic Research Program of China (973 Program), No. 2004CB518802. Authors thank Prof. Zuming Shen and Dr. Yafang Wang for their excellent technical assistance in animal experiment.

References

Crosasso, P., Ceruti, M., Brusa, P., Arpicco, S., Arpicco, S., Cattel, L., 2000. Preparation, characterization and properties of sterically stabilized paclitaxel-containing liposomes. J. Control. Release 63, 19–30.

Dhanikula, A.B., Panchagnula, R., 1999. Localized paclitaxel delivery. Int. J. Pharm. 183, 85–100.

Dosio, F., Brusa, P., Crosasso, P., Arpicco, S., Cattel, L., 1997. Preparation and characterization and properties in vitro and in vivo of a paclitaxel-albumin conjugates. J. Control. Release 47, 293–294.

Eavarone, D.A., Yu, X., Bellamkonda, R.V., 2000. Targeted drug delivery to C6 glioma by transferrin-coupled liposomes. J. Biomed. Mater. Res. 51, 10–14.

Fonseca, C., Simoes, S., Gaspar, R., 2002. Paclitaxel-loaded PLGA nanoparticles: preparation, physicochemical characterization and in vitro anti-tumoral activity. J. Control. Release 83, 273–286.

Iodoshima, N., Udagawa, C., Ando, T., Fukuyasu, H., Watanabe, H., Nakabayashi, S., 1997. Lipid nanoparticles for delivering antitumor drugs. Int. J. Pharm. 146, 81–92.

Kan, P., Chen, Z.B., Lee, C.J., Chu, L.M., 1999. Development of nonionic surfactant/phospholipid O/W emulsion as a paclitaxel delivery system. J. Control. Release 58, 271–278.

Kim, S.Y., Lee, Y.M., Baik, D.J., Kang, J.S., 2003. Toxic characteristics of methoxy poly (ethyleneglycol)/poly (epsilon-caprolactone) nanospheres; in vitro and in vivo studies in the normal mice. Biomaterials 24, 55–63.

Kratz, F., Beyer, U., 1998. Serum proteins as drug carriers of anticancer agents: a review. Drug Deliv. 5, 281–299.

Li, H., Qian, Z.M., 2002. Transferrin/transferrin receptor-mediated drug delivery. Med. Res. Rev. 22, 225–250.

Li, Y.P., Ogris, M., Wagner, E., Pelisek, J., Rüffer, M., 2003. Nanoparticles bearing polyethyleneglycol-coupled transferrin as gene carriers: preparation and in vitro evaluation. Int. J. Pharm. 259, 93–101.

Li, Y.P., Pei, Y.Y., Zhang, X.Y., Gu, Z.H., Zhou, Z.H., Yuan, W.F., Zhou, J.J., Zhu, J.H., Gao, X.J., 2001a. PEGylated PLGA nanoparticles as protein carriers: synthesis, preparation and in vivo biodistribution in rats. J. Control. Release 71, 203–211.

Li, Y.P., Pei, Y.Y., Zhou, Z.H., Zhang, X.Y., Gu, Z.H., Ding, J., Zhou, J.J., Gao, X.J., Zhu, J.H., 2001b. Stealth polycyanoacrylate nanoparticles as tumor necrosis factor-alpha carriers: pharmacokinetics and anti-tumor effect. Biol. Pharm. Bull. 24, 662–665.

Liao, W.P., DeHaven, J., Shao, J., Chen, J.X., Rojanasakul, Y., Lamm, D.L., Ma, J.K.H., 1998. Liposomal delivery of alpha-interferon to murine bladder tumor cells via transferrin receptor-mediated endocytosis. Drug Deliv. 5, 111–118.

Lundberg, B., 1997. A submicron lipid emulsion coated with amphipathic polyethylene glycol for parenteral administration of paclitaxel (taxol). J. Pharm. Pharmacol. 49, 16–21.

Mitra, A., Lin, S., 2003. Effect of surfactant on fabrication and characterization of paclitaxel-loaded polybutylcyanoacrylate nanoparticulate delivery systems. J. Pharm. Pharmacol. 55, 895–902.

Mu, L., Feng, S.S., 2002. Vitamin E TPGS used as emulsifier in the solvent evaporation/extraction technique for fabrication of polymeric nanospheres for controlled release of paclitaxel (taxol). J. Control. Release 80, 129–144.

Mu, L., Feng, S.S., 2003. A novel controlled release formulation for the anticancer drug paclitaxel (taxol): PLGA nanoparticles containing Vitamin E TPGS. J. Control. Release 86, 33–48.

Panchagnula, R., 1998. Pharmaceutical aspects of paclitaxel. Int. J. Pharm. 172, 1–5.

Pendri, P., Conover, C.D., Greenwald, R.B., 1998. Antitumor activity of paclitaxel-2′-glycinate conjugated to poly (ethyleneglycol): a water-soluble prodrug. Anti-Cancer Drug Des. 13, 387–395.

Potineni, A., Lynn, D.M., Langer, R., Amiji, M.M., 2003. Poly (ethylene oxide)-modified poly (beta-amino ester) nanoparticles as a pH-sensitive biodegradable system for paclitaxel delivery. J. Control. Release 86, 223–234.

Rodrigues, M., Carter, P., Wirth, C., Mullins, S., Lee, A., Blackburn, B.K., 1995. Synthesis and β-lactamase-mediated activation of cephalosporin-taxol prodrug. Chem. Biol. 2, 223–227.

Safavy, A., Bonner, J.A., Waksal, H.W., Buchsbaum, D.J., Gillespie, G.Y., Khazaeli, M.B., Arani, R., Chen, D.T., Carpenter, M., Raisch, K.P., 2003. Synthesis and biological evaluation of paclitaxel-C225 conjugate as a model for targeted drug delivery. Bioconjugate Chem. 14, 302–310.

Sampedro, F., Patrika, J., Santalo, P., Molins-Pujol, A.M., Bonal, J., Perez-Soler, R., 1993. Liposome as carriers of different new lipophilic antitumor drugs: a preliminary report. J. Microencapsul. 11, 309–318.

Sharma, A., Straubinger, R.M., 1994. Novel taxol formulation: preparation and characterization of taxol-containing liposomes. Pharm. Res. 11, 889–895.

Singh, M., 1999. Transferrin as a targeting ligand for liposomes and anticancer drugs. Curr. Pharm. Des. 5, 443–451.

Singla, A.K., Garg, A., Aggarwal, D., 2002. Paclitaxel and its formulations. Int. J. Pharm. 235, 179–192.

Stella, B., Arpicco, S., Peracchia, M.T., Desmaële, D., Hoebeke, J., Renoir, M., D'Angelo, J., Cattel, L., Couvreur, P., 2000. Design of folic acid-conjugated nanoparticles for drug targeting. J. Pharm. Sci. 89, 1452–1464.

Suh, H., Jeong, B., Rathi, R., Kim, S.W., 1998. Regulation of smooth muscle cell proliferation using paclitaxel-loaded poly (ethylene oxide)-poly (lactide/glycolide) nanospheres. J. Biomed. Mater. Res. 42, 331–338.

Wagner, E., Curiel, D., Cotton, M., 1994. Delivery of drugs, proteins and genes into cells using transferrin as a ligand for receptor-mediated endocytosis. Adv. Drug Del. Rev. 14, 113–136.